Increased Corrosion Resistance of Zinc Magnesium Aluminum Galvanised Coating through Germanium Additions

S.Mehraban[a], J.Malone[a], N.Lavery[a], J.Sullivan[a], D.Penney[a] S.G.R.Brown[a]

[a]Materials Research Centre, College of Engineering, Swansea University Bay Campus, College of Engineering, Fabian Way, Swansea, SA1 8EN.

The corrosion performance of a Zinc Magnesium Aluminium alloy was shown to improve through the addition of a quaternary element, Germanium. Improved corrosion resistance can be attributed to microstructural changes in the alloy due to Ge addition while in the molten state. The proportion of the most active $MgZn_2$ phase which has been shown to initiate the corrosion reaction in a ZMA alloy [1] was reduced thorough the formation of Mg2Ge crystals. The formation of crystal structures within the alloy also increased the heterogeneous nucleation of the primary zinc phase. The Scanning Vibrating Electrode Technique (SVET) was used to measure the rate of corrosion, anode life and zinc loss of the alloy samples. The results showed a zinc loss of around 50% when compared to standard ZMA alloy without Ge addition.

Introduction

Zinc, Aluminium and Magnesium (ZMA) ternary alloys are a new generation of Hot Dip Galvanised (HDG) coatings that have uses in a wide variety of markets e.g. construction and automotive. They have potential to offer similar corrosion properties as HDG coatings [2] whilst reducing the coating weight. Binary additions in HDG coatings such as additions of Al are now common. More recently there has been an expansion into tertiary additions such as magnesium. The introduction of Magnesium into Zinc Aluminium coating produces a unique microstructure which consists of primary zinc grains surrounded by: Zn-Al eutectic, Zn-Al-$MgZn_2$ ternary eutectic and $MgZn_2$ as seen in Figure 1.

Standard ZMA alloys have a carefully balanced Magnesium content (1.6 wt % Mg and 1.6 wt % Al) as lower levels of Mg have shown [2] to increase corrosion as increasing magnesium has the effect of increasing numbers of dendrites which in turn increases the Zinc corrosion initiating sites. Volvitch et al [3] has shown that ZMA alloys, with correctly balanced levels of Mg and Al, exhibit a lower corrosion rate than standard galvanised Zinc coatings (HDG) due to the formation of stable corrosion products not present on standard HDG coatings.

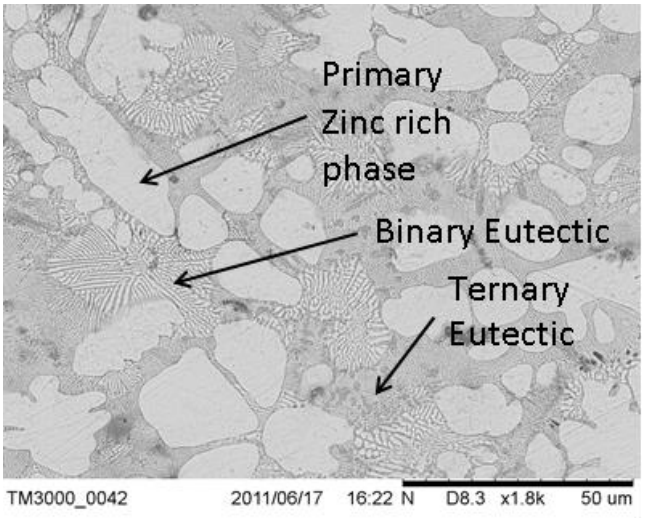

Figure 1. SEM image of a ZMA alloy, Zn-(1.6 wt% Mg)-(1.6wt% Al), the microstructure consists of primary zinc rich phase surrounded by a binary eutectic containing a lamellar of $MgZn_2$ and Zn and a ternary eutectic lamellar of $MgZn_2$, Zn and Al.

Experimental Procedure

Germanium additions were made to a ZMA master alloy consisting of 96.8% Zn, 1.6% Mg and 1.6% Al. The molten alloys were then rapid cooled using splat casting to mimic the cooling rate of a line produced galvanised coating. The samples produced were ZMA (control), ZMA 1.7 wt % Ge, ZMA 0.78 wt % Ge The composition of each sample alloy was measured through cast analysis using ICP-MS, and EDS analysis.

The technique employed to quantify the corrosion resistance of novel quaternary additional alloys was the Scanning Vibrating Electrode Technique (SVET). SVET is a method of investigating the localised corrosion activity above a surface and allows a quantitative assessment of performance of the alloys. The SVET vibrates a scanning micro tip electrode relative to the scanned surface at a constant amplitude and frequency. The micro tip registers an alternating potential generated chemically by the ionic current flux passing through the electrolyte. The SVET signal is directly proportional to the ionic current density and thus the corrosion activity.

Results and discussion

Phase analysis.

EDS analysis was used to identify the elemental proportions each phase and SEM image analysis to quantify the percentage proportion of the phases present. It is clear that the additions of germanium and the creation of Magnesium Germainide have a profound effect on the microstructure of ZMA alloys. The formation of Magnesium Germainide at high temperatures controls the growth of both primary phase and eutectics as well as the

constituents of the eutectic. The growth mechanism is observed to be similar to the formation of Mg2Si [3].

When alloying pure Ge to the ZMA alloy the Ge was heated to 1200°C (T_m= 938°C) and ZMA was heated separately to 650°C, when liquid Ge was combined with the ZMA the first phase to form was Mg2Ge (T_m=1115°C). Mg2Ge forms in a kinetic growth manner when there is a high latent heat of fusion and as Ge has a high affinity for Mg it removes the magnesium from the liquid alloy. Zn rich phase heterogeneously forms around the solid Mg_2Ge nucleation points and finally the eutectic forms. The amount of germanium added to the system dictates the remaining microstructure.

Phase identification

Phases present in ZMA. The phases produced in splat cast ZMA can be seen to be the same as standard ZMA alloy of the galvanised line; there is a Zn rich phase (Figure 2), a binary Zn-MgZn2 lamellar eutectic (Figure 3) and a fine Zn, Al and MgZn2 ternary eutectic (Figure 4). The binary phase contains approximately 91.51 Wt % Zn and 7.16 Wt % Mg. The ternary contains 88.44 Wt % Zn, 7.19 Wt % Al and 4.37 Wt % Mg. This shows that there is an Mg rich eutectic and an Al rich eutectic present.

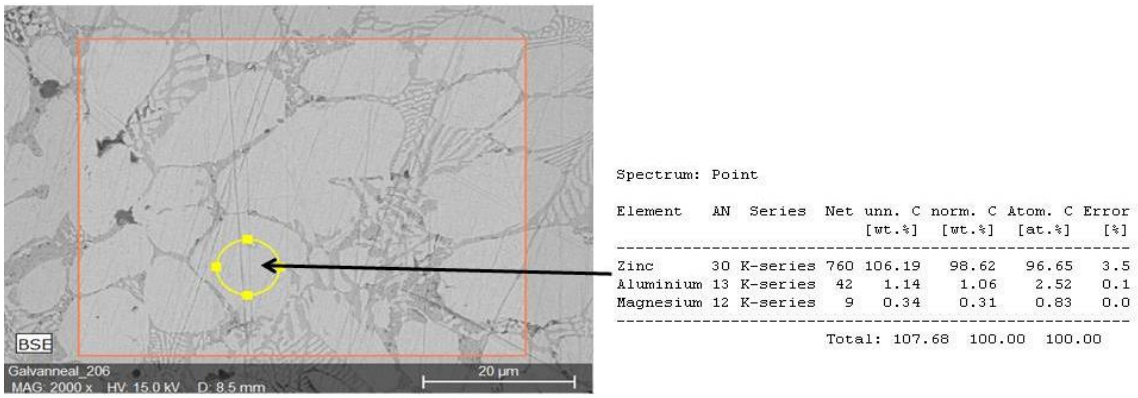

Figure 2. ZMA Zn Rich phase

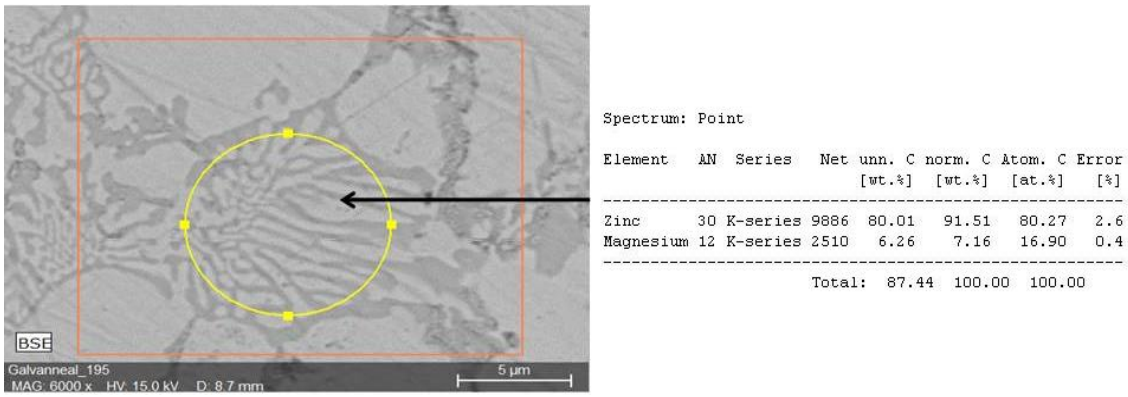

Figure 3. ZMA binary eutectic

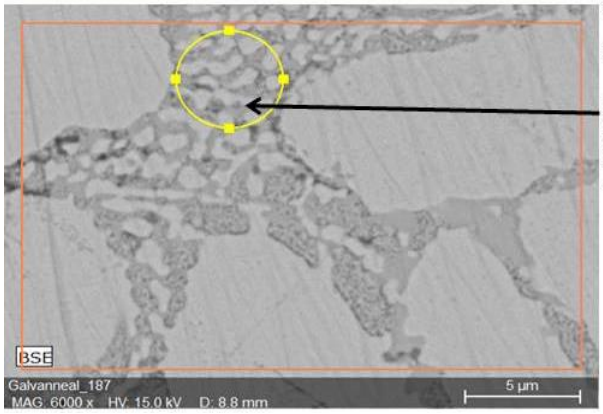

Spectrum: Point

Element	AN	Series	Net unn. C [wt.%]	norm. C [wt.%]	Atom. C [at.%]	Error [%]
Zinc	30	K-series	2750	83.43	88.44	75.19	2.8
Aluminium	13	K-series	1094	6.78	7.19	14.81	0.3
Magnesium	12	K-series	485	4.12	4.37	10.00	0.2
Total:				94.33	100.00	100.00	

Figure 4. ZMA ternary eutectic

Phases present ZMA 0.78% Ge. The Mg2Ge crystals are fully formed octahedral crystals (Figure 5) opposed to the hopper crystals observed in ZMA 1.7 Wt % Ge (Figure 8). The amount of Ge is less than the higher 1.7 Wt % Ge alloy therefore the crystals formed do not use up the majority of the Mg and form smaller crystals. The growth of the {111} face is not restricted therefore the crystals are also fully formed. This could be attributed to a slower cooling rate as the growth of the crystals does not remove as much surface energy as the larger crystals in the ZMA 1.7 Wt % Ge alloy.

The Zn rich phase (Figure 6) found in the ZMA 0.78 Wt % Ge is the same as what is observed in all ZMA alloys at 98.96 Wt % Zn with 1.04 Wt % Al. As with the ZMA 1.7 Wt % Ge sample the crystals are surrounded by the Zn rich phase suggesting that the Zn rich phase nucleates from the Mg2Ge formations.

The eutectic phases vary compared to the eutectic phase observed in standard ZMA alloy; both eutectics are ternary and there is no Mg rich eutectic and there is no fine nodular Al rich ternary. There are two types of eutectics in the ZMA 0.78 Wt % Ge alloy (Figure 61); the lamellar (figure 7) consists of a ternary eutectic containing Zn (89.76 Wt % Zn), Al (5.62 Wt % Al) and Mg (4.63 Wt % Mg). The second ternary eutectic contains Zn (88.60 Wt % Zn), Al (7.13 Wt % Al) and Mg (4.27 Wt % Mg). The ternary eutectic appears to be a lamellar with Al nodules and as such there is a higher Al content compared with the lamellar Eutectic. The Mg content in the eutectics is higher than the Mg content in the eutectic of the ZMA 1.7 Wt % Ge and would be expected as the formation of the Mg2Ge does not completely remove the Mg from the remaining microstructure meaning there is remaining Mg available for eutectic formations. The removal of Mg and formation of Mg2Ge could also explain why the eutectics differ from the eutectics found in the standard ZMA alloy as cooling rates are faster, reducing diffusion, and there is less Mg available for eutectic formation.

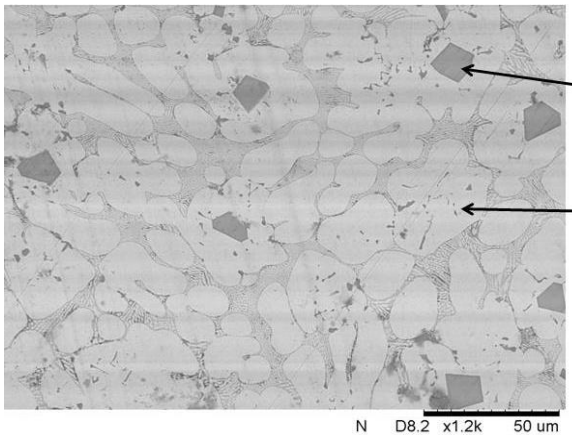

Figure 5. ZMA 0.78 Wt % Ge Mg2Ge Formations

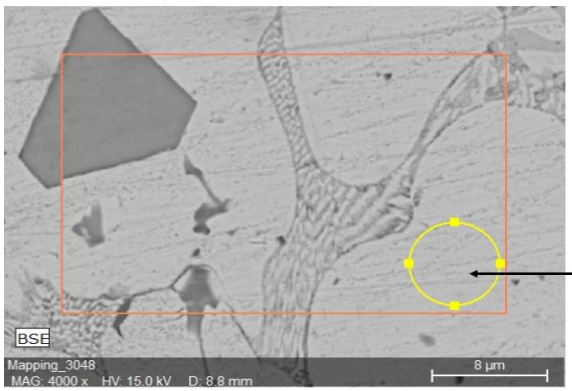

Spectrum: Point

Element	AN	Series	Net	unn. C [wt.%]	norm. C [wt.%]	Atom. C [at.%]	Error [%]
Zinc	30	K-series	4031	87.33	98.96	97.52	2.9
Aluminium	13	K-series	207	0.92	1.04	2.48	0.1
Germanium	32	L-series	0	0.00	0.00	0.00	0.0
Magnesium	12	K-series	0	0.00	0.00	0.00	0.0
Total:				88.25	100.00	100.00	

Figure 6. EDS Analysis showing Zn Primary phase of ZMA 0.78 Wt % Ge

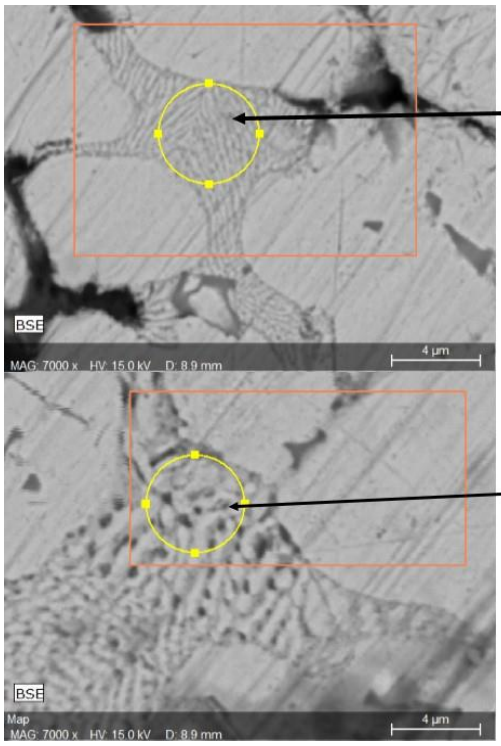

Element	AN	Series	Net	unn. C [wt.%]	norm. C [wt.%]	Atom. C [at.%]	Error [%]
Zinc	30	K-series	8687	84.13	89.76	77.50	2.8
Aluminium	13	K-series	2370	5.26	5.62	11.75	0.3
Magnesium	12	K-series	1423	4.34	4.63	10.75	0.3
Total:				93.73	100.00	100.00	

Element	AN	Series	Net	unn. C [wt.%]	norm. C [wt.%]	Atom. C [at.%]	Error [%]
Zinc	30	K-series	2029	77.85	88.60	75.49	2.6
Aluminium	13	K-series	782	6.26	7.13	14.72	0.3
Magnesium	12	K-series	341	3.75	4.27	9.78	0.2
Total:				87.87	100.00	100.00	

Figure 7. EDS analysis showing the eutectic phase of ZMA 0.78 Wt % Ge

Phases present in ZMA 1.7% Ge. The first phase to form in the alloy is the magnesium germanide formations as discussed previously (5.2.1). They form hopper crystals and partially formed crystals (Figure 8). The crystals are much larger than the crystals found on the ZMA 0.78 Wt % Ge (Figure 5 and Figure 6) and there are also no fully formed crystals. This is possibly due to the increasing amount of germanium using up more magnesium which leads to larger crystals. The larger growth could possibly remove more surface energy slowing down growth on the {111} face of the crystals. By the time the crystals are ready to be fully formed they may not be able to diffuse out the aluminium that blankets the {111} face and therefore restricting the growth [3].

Figure 9 shows the Zn rich phase in the ZMA 1.7 Wt % Ge alloy as 98.59 Wt % Zn with a small amount of Al (1.41 Wt %). The Mg2Ge crystals are found in the Zn rich phase suggesting that the zinc rich phase nucleates from the solid crystals when cooling.

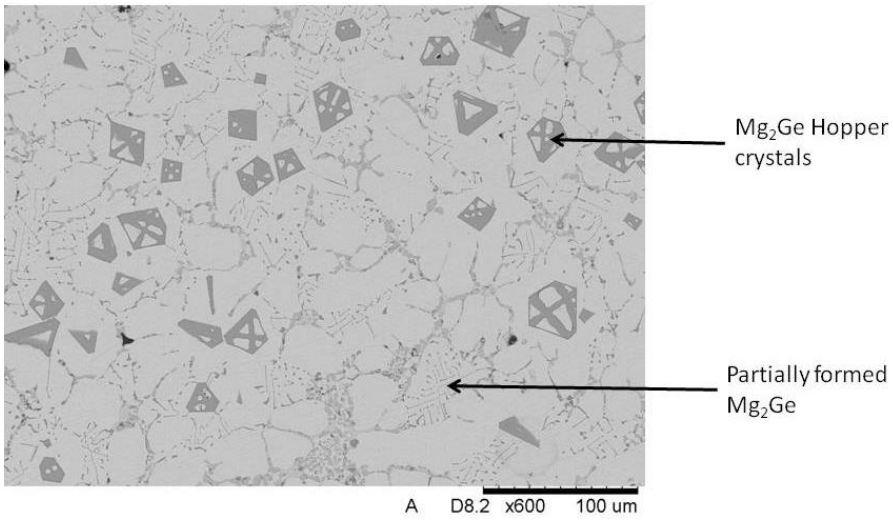

Figure 8. ZMA 1.7 Wt % Ge Mg2Ge formations

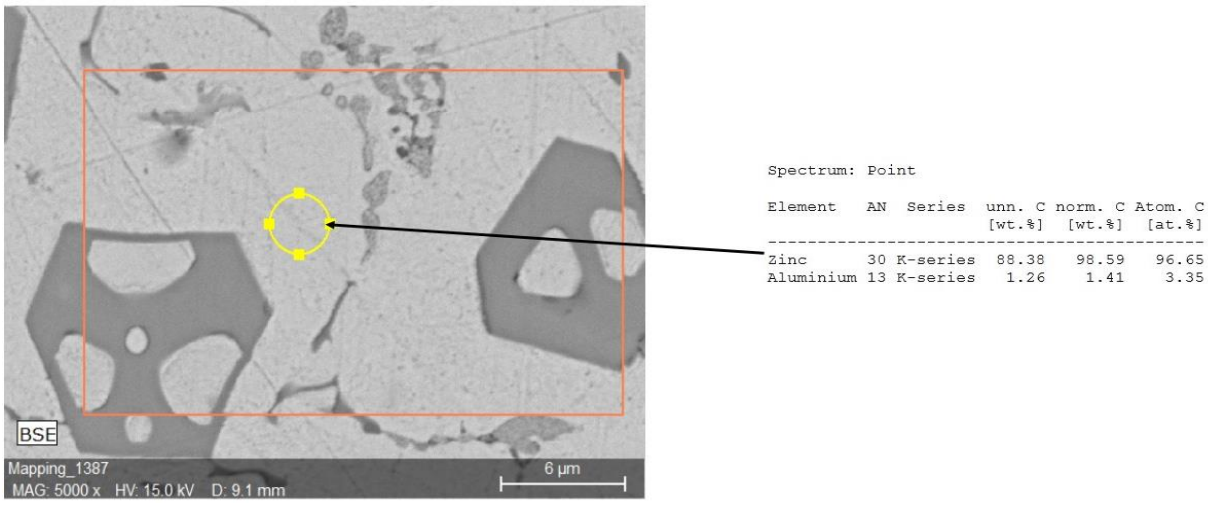

Figure 9. EDS analysis of zinc rich phase in ZMA 1.7 wt % Ge alloy

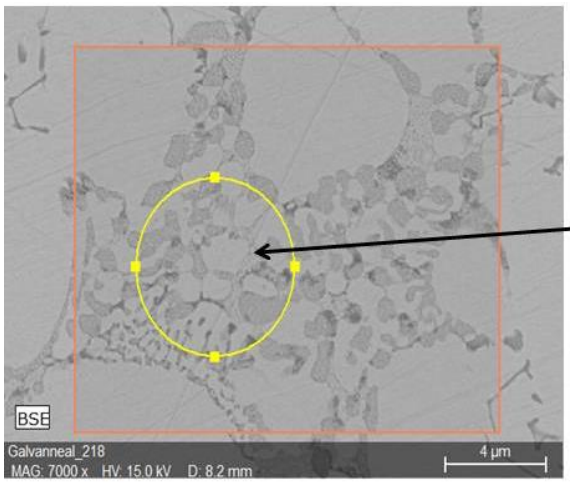

Spectrum: Point

Element	AN	Series	Net unn. C [wt.%]	norm. C [wt.%]	Atom. C [at.%]	Error [%]
Zinc	30	K-series	6951	81.56	88.53	75.74	2.7
Aluminium	13	K-series	3305	8.67	9.41	19.51	0.4
Magnesium	12	K-series	520	1.90	2.06	4.75	0.1
Total:			92.13	100.00	100.00		

Figure 10. Eutectic phase observed in ZMA 1.7 Wt % Ge

Proportional Phase Analysis Representative micrograhs were selected and image analysis allowed each sample's phases to be quantified and the changes in the phases tracked. Each observed phase was highlighted using Photoshop CS6 and then the area determined using 'Sigmascan' image anlysis software.

By comparing the primary phase present it is clear that primary phase increases with additions of Ge (Figures 12,13); this could be due to the increased nucleation points allowing the primary phase to increase. The Zn rich phase is far higher at ZMA 1.7 Wt % than any other samples. This could be due to the increase in Ge removing Mg available for eutectic reactions and causing faster cooling rates resulting in smaller eutectic areas.

Conversely as Ge is added the amount of available eutectic is reduced from 30% in standard ZMA alloy to 5% in ZMA 1.7 Wt % Ge (Figure 13). This can be attributed to the removal of Mg, increase in nucleation of Zn rich phase and increase in cooling rates.

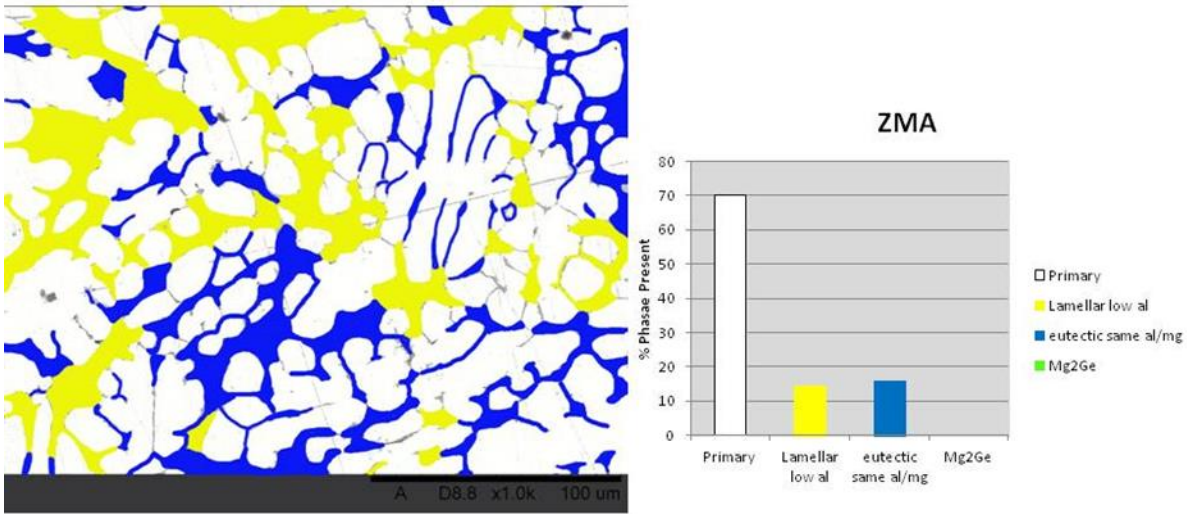

Figure 11. Phase analysis of ZMA alloy Standard ZMA alloy (Figure 70) has around 70 % primary phase with a 14 % binary and 16 % ternary eutectic.

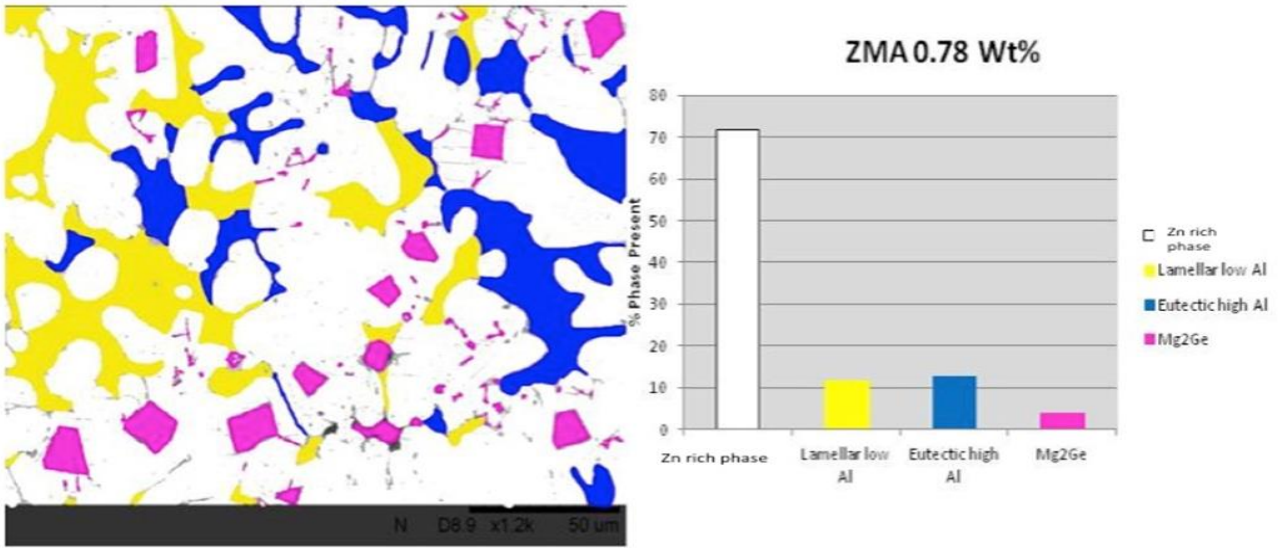

Figure 12. Phase analysis of ZMA 0.78 Wt % Ge7. Figure 72 shows the phases present in ZMA 0.78 Wt % Ge. The Zn phase represents 72 %, the Mg rich lamellar represents 12 % and Al rich ternary 13 %. The Mg2Ge Phase makes the remainder of 4%.

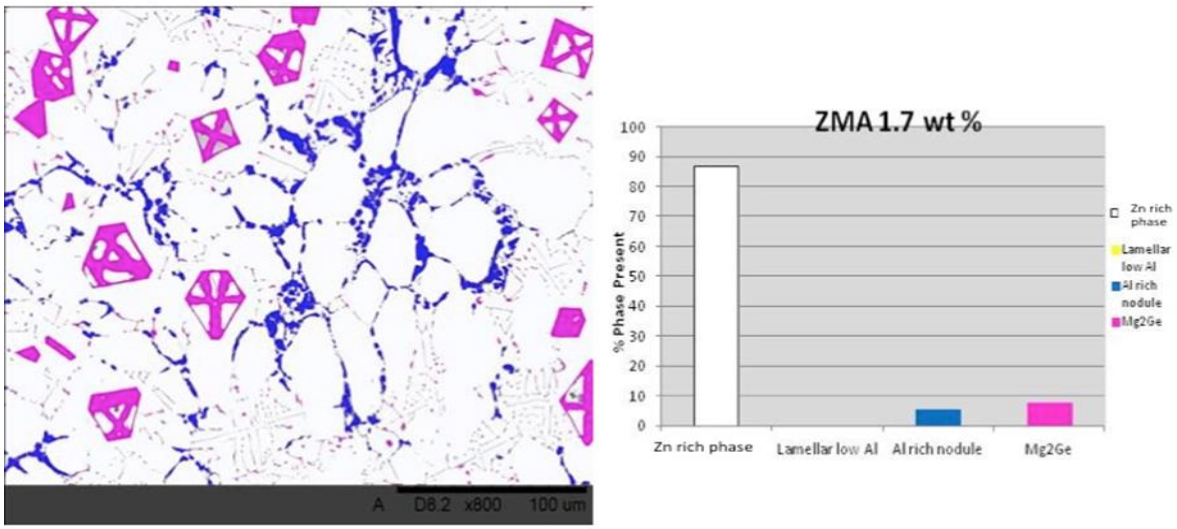

Figure 13. Phase analysis of ZMA 1.7 Wt % Ge With additions of 1.7 Wt % Ge (Figure 71) the Zn rich phase represents 88%, there is no lamellar low Al eutectic and the ternary eutectic which is Al rich only represents 5%. Due to the large additions of Ge the Mg2Ge phase is 8%.

Corrosion testing

The Scanning vibrating electrode technique (SVET) was used to assess the corrosion performance of ZMA 1.7 Wt % Ge, 0.78 Wt % Ge and compared with standard ZMA. The results (Figure 14) shows that ZMA 0.78 Wt% Ge performed the best an average

of 3.4 gm-2 of mass loss which compared with standard ZMA (7.5 gm-2), ZMA 1.7 Wt % Ge only performs marginally better with an average of 7 gm-2. A standard hot dip galvanised coating (99.8 wt% Zn 0.2 wt% Al) was tested as a bench mark. it is clear that with an average mass loss of 10.97 gm-2 the corrosion performance is worse than that of standard ZMA .

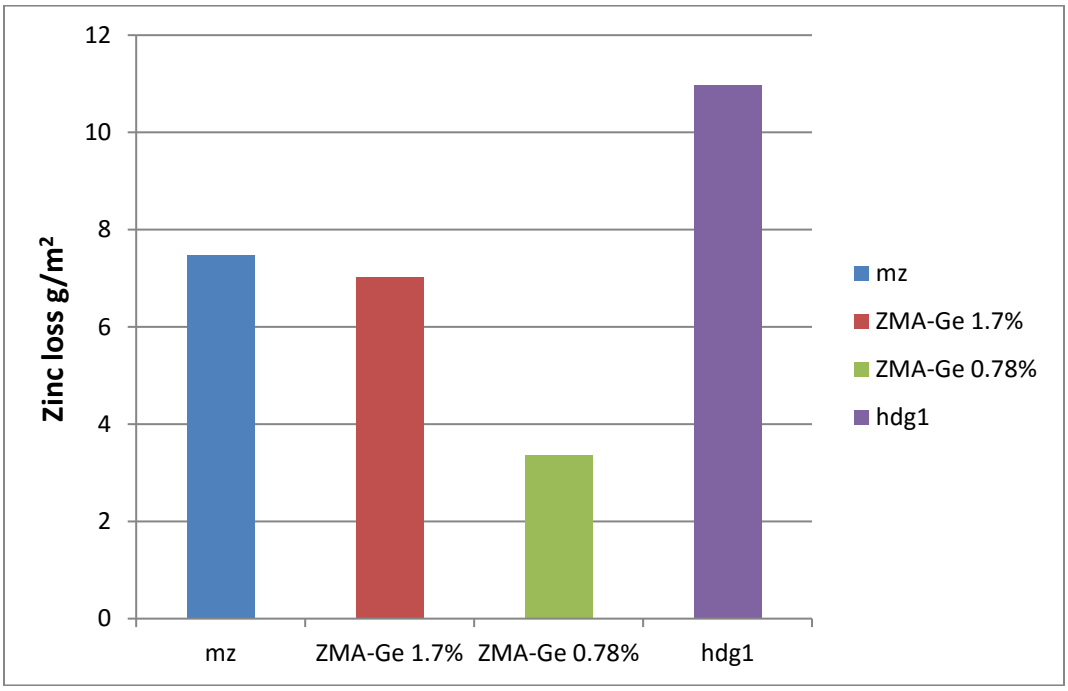

Figure 14. Zinc mass loss of ZMA alloys with varying additions and HDG over 24 hours.

It has been shown in previous work [1] that initial microstructural attack in ZMA alloys begins on the $MgZn_2$ phase within the eutectic phase, production of hydroxide ions at the cathode and potential hydrolysis of metal ions at the anode sets up a pH gradient. A corrosion product ring forms due to the flow of metal ions to the cathode and hydroxide ions to the anode. Where they meet an insoluble salt is formed and then Cl^- ions build up around the anodic area which this leads to the de-alloying of binary and ternary eutectics and finally, attack of primary Zn phase. In terms of the protection mechanism typically magnesium ions form stable precipitates of magnesium hydroxide $Mg(OH)_2$ on cathodes, which limit the oxygen reaction at the cathodes which lowers the general activity [4]. In chloride environments Simonkolleite (Zn5(OH)8Cl2H2O) tends to form close to the anodic sites and the presence of Al^{3+} ions stabilise simonkolleite against transformations into ZnO or Zinc hydroxycarbonate (Zn5(CO3)2(OH)6). Although it has been shown that the corrosion products of standard ZMA alloy depend largely upon the conditions in which they are corroded, in normal conditions Zinc hydroxycarbonate and simonkolleite are formed [5],[6]. The result is a corrosion resistant coating that corrodes less than standard Zn coatings. Aluminium in the eutectic breaks down to form Al_2O_3 which is a poor cathode and reduces cathodic activity. It has been shown that magnesium germanide breaks down in H_2O to form germanium hydride and MgO and as the hydride is volatile the surface is then coated with MgO [7].

Therefore by adding large quantities of Ge (ZMA 1.7 Wt % Ge) where Mg is removed from the eutectic and sequestered into Mg2Ge the protection mechanism changes. There is no magnesium hydroxide to protect the eutectic however there is Al_2O_3 but as the eutectic area is minimal (5.6 % in ZMA 1.7 Wt % Ge) it cannot protect the entire surface. Although Mg2Ge breaks down to form MgO it will only form where the crystals are located, 8.5% of the microstructure in ZMA 1.7 Wt % Ge, therefore the surface is relying mainly on ZnO for protection. Although the overall Zinc loss is marginally less than ZMA, which could relate to a slower initiation for corrosion as Mg is tied up in the more stable Mg2Ge form.

ZMA 0.78 Wt % Ge performs twice as well as Standard ZMA, ZMA 1.7 Wt % Ge and three times better than HDG this could be due to finding the correct levels of Mg in the eutectic to provide a magnesium hydroxide protective layer, a mainly aluminium eutectic which breaks down to form Al_2O_3, the added effect of MgO from the Mg2Ge crystal formations and the reduced eutectic size compared to the ZMA coating. The net result is a less initially active eutectic than ZMA that still provides the protective coatings of corrosion products associated with ZMA alloys which suppress corrosion over the duration of the test. Elvins [8] found that increasing Mg concentrations led to an increase in primary Zn size and as such, an increase in corrosion rate. The Zn rich phase amount in ZMA 0.78 Wt % Ge is roughly 72 % which is close to ZMA (70%). However compared with ZMA 1.7 Wt % Ge (88%) the Zn rich phase is 16 % lower in ZMA 0.78 Wt % Ge which could also explain the increased corrosion performance.

To further explore this hypothesis, corrosion maps from the SVET investigations were compared between ZMA, ZMA 1.7 Wt % and ZMA 0.78 Wt % Ge maps. The corrosion activity was normalised to the most active scale of current density distribution which allows direct comparison between samples. They can be seen from Figure 15 to Figure 19 which shows the corrosion at zero hours and every six hours thereafter till the experiment finishes at twenty four hours.

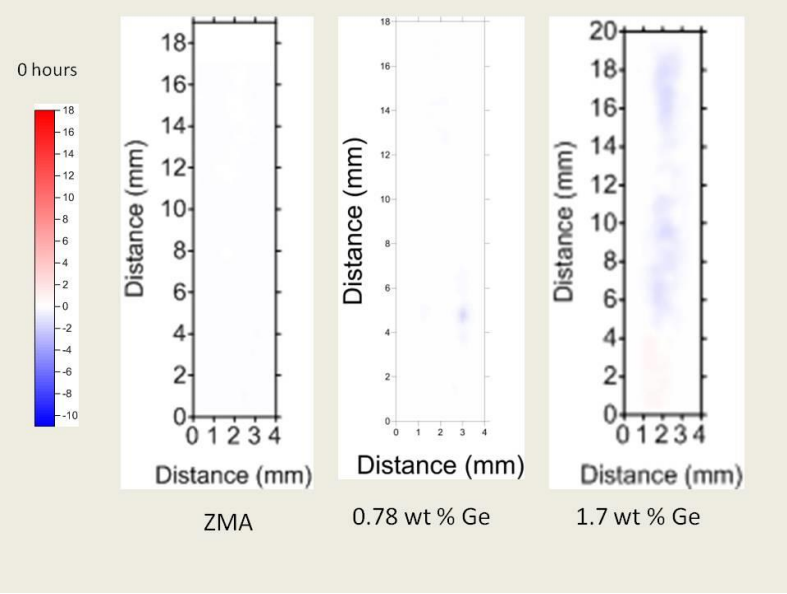

Figure 15. Corrosion plots at 0 Hrs

Initially ZMA 1.7 Wt % Ge appears more active (Figure 15), with large areas of cathodic activity (blue) this has to be balanced by anodic activity. There are some small areas of cathodic activity in ZMA and ZMA 0.78 Wt % but very small when compared to ZMA 1.7 Wt % Ge.

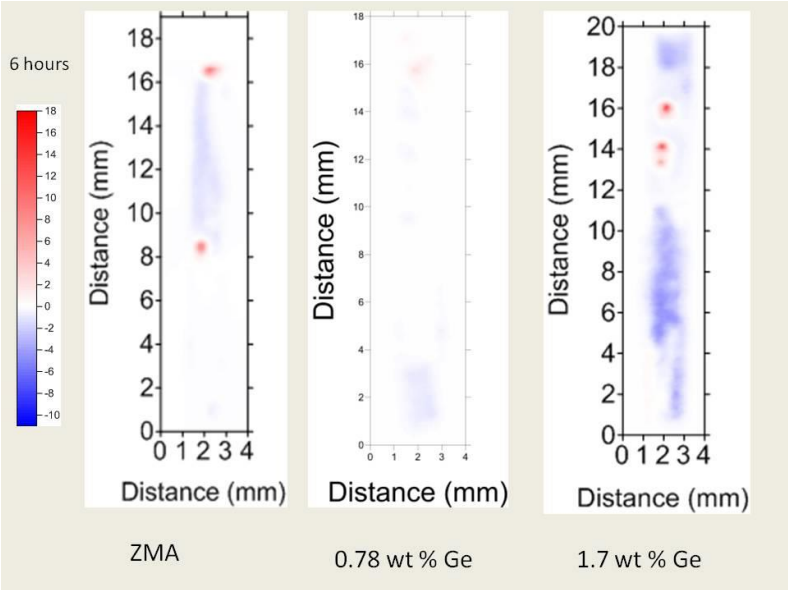

Figure 16. Corrosion plots at 6 Hrs

At 6 hours (Figure 16) again ZMA 1.7 Wt % Ge is more active both cathodically and anodically; small localised anodic areas can be seen (red). ZMA is showing signs of cathodic region with some small localised anodic regions which are similar to ZMA 1.7 Wt % Ge. ZMA 0.78 Wt % Ge shows little signs of activity with no localised anodic areas.

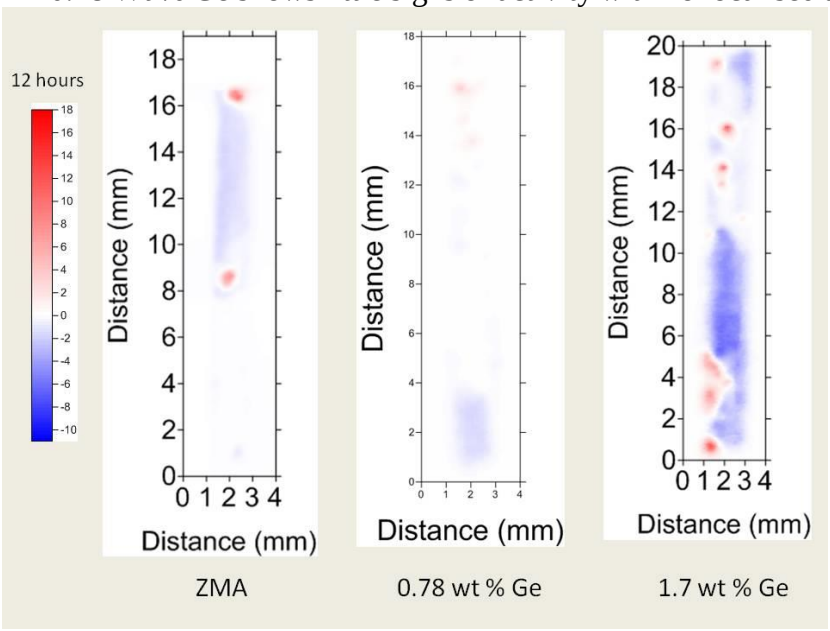

Figure 17. Corrosion plots at 12 Hrs

After 12 hours (Figure 17) of corrosion ZMA 1.7 Wt % Ge appears to be increasing in activity with darker blue regions of cathodic activity and an increase in localised anodic sites. The ZMA alloy activity seems to show cathodic and anodic activity similar to the

activity seen at 6 hours. ZMA 0.78 Wt % Ge activity does not seem to be any more intense than at 6 hours and is significantly lower than ZMA and ZMA 1.7 Wt % Ge.

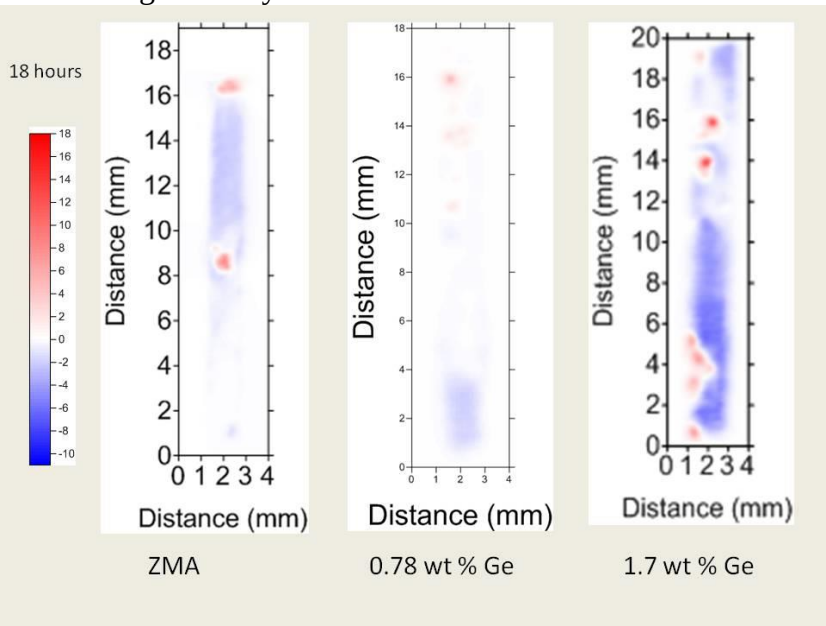

Figure 18. Corrosion plots at 18 Hrs

The corrosion maps at 18 hours (Figure 18) shows that the anodic sites on ZMA 1.7 Wt % are well established as with the anodes on ZMA. The corrosion intensity levels seem to have levelled off in both samples. There are signs of localised corrosion on ZMA 0.78 Wt % Ge although they are both less than ZMA and ZMA 1.7 Wt % Ge.

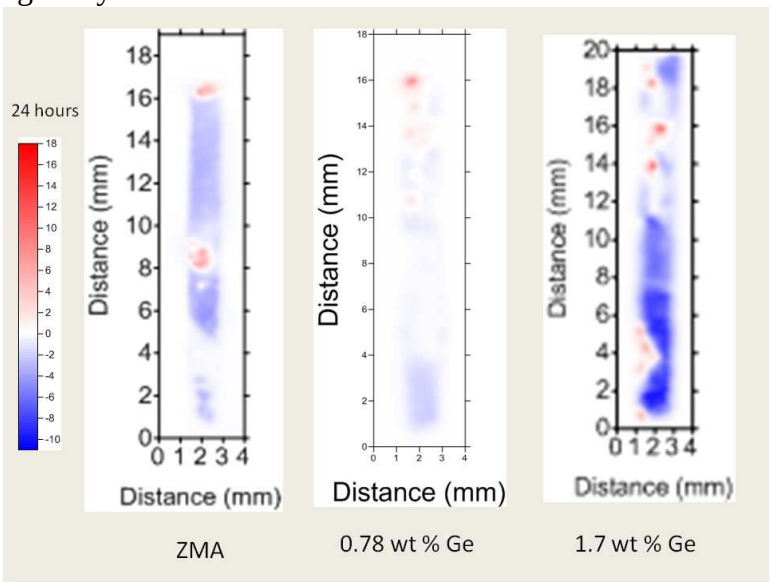

Figure 19. Corrosion plots at 24 Hrs

After 24 hours (19) is similar to that at 18 hours i.e. strong cathodic regions with established anodes in ZMA 1.7 Wt % Ge and weaker cathodic and established anodes in ZMA. There are signs of stronger anodic regions with ZMA 0.78 Wt % Ge.

Although in this instance ZMA 1.7 Wt % Ge is more active this is a singular result and over an average it was only marginally better than standard ZMA. It backs up the

hypothesis that ZMA 1.7 Wt % Ge cannot suppress the cathodic reaction as well as ZMA 0.78 Wt % Ge therefore once initiated there is little to prevent further degradation. The maps also show that corrosion is very much suppressed on the surface of ZMA 0.78 Wt % Ge which could be due to the suppression of the cathode which leads to a less reactive coating.
By looking at the average corrosion rates results it displays a quantitative assessment of the corrosion performance of the alloys with respect to time.

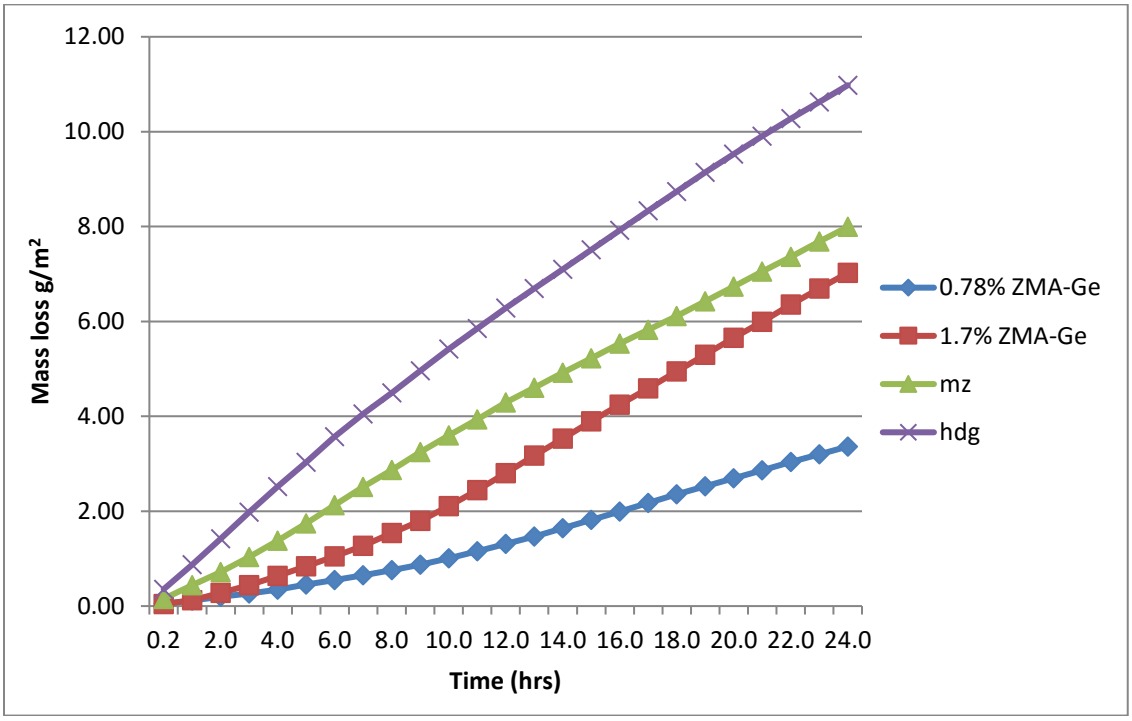

Figure 10. Mass loss rate of ZMA with varying additions and HDG.

Figure 20 shows the corrosion rate of HDG, ZMA, ZMA 0.78 WT % Ge and ZMA 1.7 Wt % Ge over a 24 hour period. The results are based on an average of three experiments and show trends that match the hypothesis. ZMA 0.78 Wt % Ge corrosion rate is slow to start and the corrosion is suppressed giving low overall mass loss. ZMA 1.7 Wt % Ge is slow to start however once corrosion is initiated it quickly ramps up to rates quicker than that of ZMA. ZMA has a steady corrosion rate throughout the experiment although it is initially higher than both ZMA 1.7 Wt % Ge and ZMA 0.78 Wt % Ge.

Conclusions

SVET was used to analyse the corrosion behavior of ZMA alloys with addition of Ge. Samples of ZMA 1.7 Wt Ge, 0.78 Wt % Ge and HDG were compared with standard ZMA.

SVET results showed that additions of 1.7 Wt % Ge only reduced mass loss from 7.4 gm-2 in ZMA to 7 gm-2. However at Ge levels of 0.78 Wt % Ge corrosion was reduced by over half to 3.4 gm-2. This could be due to a number of reasons: at higher levels (1.7 Wt % Ge) there is barely any eutectic and the eutectic that remains has no Mg in it as the Mg is removed by the formation of the Germanide crystals and eutectics. The result is the

corrosion products that are usually associated with the improved corrosion resistance of ZMA alloys (stable Simonkolleite, hydroxycarbonate, and magnesium hydroxide) are less prevalent being that the area of eutectic is so small and does not contain much magnesium. Magnesium germanide only breaks down to form MgO which isn't enough to prevent corrosion and corrosion isn't cathodically suppressed. The result is that although corrosion has shown to take some time to initiate once it is initiated there are insufficient corrosion products to reduce the corrosion rate.

At levels of 0.78 Wt % Ge superior corrosion performance was observed. This could be due to a favorable ratio of eutectics and its constituents i.e. there is enough of a eutectic area to provide corrosion protection from stabilised simonkolleite, hydroxyl carbonate and magnesium hydroxide whilst keeping the magnesium levels in the eutectic to a minimum so corrosion takes a sometime to initiate and when it does it is suppressed. There is an added effect of aluminium oxide being more prevalent as by weight percentage there is more aluminium than magnesium in the eutectic. The end result of this is the cathodic reaction is suppressed, as the corrosion products formed are poor cathodes, and the corrosion rate is suppressed. This can be seen from lower corrosion rates and a reduced corrosion potential.

Standard hot dip galvanised zinc (HDG) was tested to see if the removal of Mg was important, the result (10.7 gm-2) Zinc loss for HDG compared to (7.5 gm-2) for standard ZMA showed that standard ZMA without its altered chemistry offers improved corrosion resistance over HDG, and thus magnesium is desirable in the microstructure.

Acknowledgements

The authors would like to thank the Welsh Government, particularly, the A4B team who made the funds available to the set-up the Materials Advanced Characterisation Centre (MACH1) laboratories at Swansea University.

References

[1] J. Sullivan, S. Mehraban, and J. Elvins, "In situ monitoring of the microstructural corrosion mechanisms of zinc–magnesium–aluminium alloys using time lapse microscopy," *Corros. Sci.*, vol. 53, no. 6, pp. 2208–2215, Jun. 2011.

[2] J. Elvins, J. A. Spittle, and D. A. Worsley, "Relationship between microstructure and corrosion resistance in Zn–Al alloy coated galvanised steels," *Corros. Eng. Sci. Technol.*, vol. 38, no. 3, pp. 197–204, Sep. 2003.

[3] C. Li, Y. Y. Wu, H. Li, and X. F. Liu, "Morphological evolution and growth mechanism of primary Mg2Si phase in Al–Mg2Si alloys," *Acta Mater.*, vol. 59, no. 3, pp. 1058–1067, Feb. 2011.

[4] E. Diler, B. Rouvellou, S. Rioual, B. Lescop, G. Nguyen Vien, and D. Thierry, "Characterization of corrosion products of Zn and Zn-Mg-Al coated steel in a marine atmosphere," *Corros. Sci.*, vol. 87, pp. 111–117, 2014.

[5] N. LeBozec, D. Thierry, M. Rohwerder, D. Persson, G. Luckeneder, and L. Luxem, "Effect of carbon dioxide on the atmospheric corrosion of Zn–Mg–Al coated steel," *Corros. Sci.*, vol. 74, no. 0, pp. 379–386, Sep. 2013.

[6] N. LeBozec, D. Thierry, A. Peltola, L. Luxem, G. Luckeneder, G. Marchiaro, and

M. Rohwerder, “Corrosion performance of Zn-Mg-Al coated steel in accelerated corrosion tests used in the automotive industry and field exposures,” *Mater. Corros.*, vol. 64, no. 11, pp. 969–978, 2013.

[7] H. R. Shanks, “The growth of magnesium germanide crystals,” *J. Cryst. Growth*, vol. 23, no. 3, pp. 190–194, 1974.

[8] J. Elvins, J. Spittle, J. Sullivan, and D. Worsley, “The effect of magnesium additions on the microstructure and cut edge corrosion resistance of zinc aluminium alloy galvanised steel,” *Corros. Sci.*, vol. 50, no. 6, pp. 1650–1658, Jun. 2008.